Heliyon 10 (2024) e30851

Contents lists available at ScienceDirect

Heliyon

journal homepage: www.cell.com/heliyon

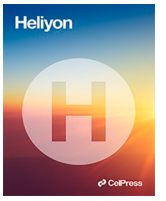

Research article

Micro-shear bond strength of a novel resin-modified glass ionomer luting cement (eRMGIC) functionalized with organophosphorus monomer to different dental substrates

Rabeia J. Khalil *, Abdulla M.W. Al-Shamma

Department of Restorative and Aesthetic Dentistry, College of Dentistry, University of Baghdad, Baghdad, Iraq

ARTICLE INFO

Keywords:
Luting resin cement
Microshear bond strength
Phosphate functional monomers
Resin-modified glass ionomer luting cement

ABSTRACT

Objectives: This study aims to assess and compare the micro-shear bond strength (μSBS) of a novel resin-modified glass-ionomer luting cement functionalized with a methacrylate co-monomer containing a phosphoric acid group, 30 wt% 2-(methacryloxy) ethyl phosphate (2-MEP), with different substrates (dentin, enamel, zirconia, and base metal alloy). This assessment is conducted in comparison with conventional resin-modified glass ionomer cement and self-adhesive resin cement.

Materials and methods: In this *in vitro* study, ninety-six specimens were prepared and categorized into four groups: enamel (A), dentin (B), zirconia (C), and base metal alloys (D). Enamel (E) and dentin (D) specimens were obtained from 30 human maxillary first premolars extracted during orthodontic treatment. For zirconia and metal alloys, 48 disks were manufactured using IPS e.max ZirCAD through dry milling and Co–Cr powder alloy by selective laser milling. Each group was further subdivided into three subgroups (n = 8) according to the luting cement used: (1) Fuji PLUS resin-modified glass ionomer luting cement (FP) as a control cement, (2) modified control cement (eRMGIC), and (3) RelyX U 200 (RU 200) self-adhesive resin cement. The two-way analysis of variance and Tukey's HSD were used to assess the data obtained from measuring the μSBS of the samples.

Results: The results of this study showed that the mean μSBS values of eRMGIC were statistically higher compared to FP in all tested groups ($p < 0.001$). The mean μSBS results of eRMGIC were non-significantly different from those recorded by RU 200 for all substrates except for the dentin substrate, where the RU200 cement produced significantly higher strength ($p < 0.001$). The failure modes were limited to a combination of mixed and adhesive failures without pure cohesive failure.

Significance: The functionalization of FP with an organophosphorus co-monomer (2-MEP) directly affects the adhesion performance of the functionalized cement, which may be utilized to develop a new type of acid-base cement. It exhibited a performance comparable to that of resin-based cement and should serve well under different clinical conditions.

* Corresponding author.
E-mail address: rabeea.jassem1104a@codental.uobaghdad.edu.iq (R.J. Khalil).

https://doi.org/10.1016/j.heliyon.2024.e30851
Received 3 December 2023; Received in revised form 27 March 2024; Accepted 7 May 2024
Available online 7 May 2024

1. Introduction

Indirect restorations are bonded to tooth surfaces using luting cement, which locks the restoration mechanically in place by filling the microscopic gaps between the tooth structure and restoration [1]. Luting materials provide chemical bonding, mechanical interlocking, or a combination of these techniques for retaining indirect restorations. The conventional cementation method depends primarily on the friction generated between the surfaces of the prepared tooth and the fitting walls of the restorations [2]. Modern materials use micromechanical and chemical adhesion to bond cement, tooth surfaces, and artificial restorations [3].

To ensure the quality of the cementation process, it is essential to have a comprehensive understanding of the properties and clinical applications of luting agents. A strong seal between the restoration and teeth is achieved using luting agents, which not only holds the restoration in place but also prevents microleakage and cavity formation on the surface. Therefore, luting materials affect the duration of indirect restorations [4].

The optimal luting cement should possess excellent tensile, shear, and compressive strengths to effectively endure the stress experienced during contact between the restoration and tooth. Generally, it could be the weakest link in the tooth-cement-restoration chain used in permanent prosthodontic therapy; however, to date, no luting material has been developed with all of the qualities of an ideal cement [5].

Among the luting cements, GIC was commonly used due to its bonding property to the tooth structure which was achieved by chemical bonding of its carboxylic constituents with the calcium present in the enamel and dentin [6,7]. GIC has a low binding strength with dentin owing to the aforementioned adhesion process [8]. This fragility arises in part from the tendency of the smear layer to fail cohesively, which can impede the adhesion mechanism [9].

The inclusion of monomer molecules in GICs creates a hybrid material, a new type of GIC called the RMGIC [10,11]. The development of the RMGIC was aimed at improving the working time and handling properties of a standard GIC, the physical features of GICs were enhanced by these adjustments [10]. The polymerization of RMGIC occurs in two stages: stage one is accelerated by exposure to light or chemicals, and stage two begins as soon as the powder and liquid are mixed and continues for up to 24 h [12,13].

By contrast, compared to traditional GICs, the resin component of RMGICs amplifies the effects of polymerization shrinkage. Polymerization shrinkage may result in gap development, potentially leading to microleakage and subsequent postoperative sensitivity, secondary caries, and loss of adhesion, as widely reported in the literature [14]. Water sorption may reduce the contraction gap but can impair the ability of the material to seal initially, thereby reducing the efficacy of the seal [15].

The advent of the self-adhesive resin cements (SARCs) has facilitated significant advancements. For instance, etching, priming, and bonding no longer need to be performed separately. SARCs are formulated using innovative compositions of monomers, initiators, and fillers [3].

The acidic monomers of these cements (acidic methacrylates) can interact with essential luting cement fillers and the hydroxyapatite (HAp) crystals of dental hard tissue, using their multifunctional phosphate groups [16]. In recent studies, SARCs have exhibited a higher bonding strength than RMGICs for various materials, including aluminum oxide ceramics, non-noble and noble metals, and pressable ceramics [17].

Owing to their multifunctional phosphoric acid methacrylates, self-etching resin cements appear to facilitate adequate attachment to various substrates [18]. Zr restorations can also be bonded using functional monomers induced in adhesive resin cements, such as 11-methacryloyloxundecan 1,1-dicarboxylic acid (MAC-10),4-methacryloxyethyl trimellitate anhydride (4-META), and 10-methacryloyloxydecyl dihydrogen phosphate (MDP) [19]. These monomers bond chemically with surfaces composed of Zr, noble metals, and non-noble metals, thereby promoting enhanced, enduring, and robust bond strength [20].

Luting indirect restorations with RMGIC is common practice, however it doesn't have the adhesive properties of resin based cements, which could compromise the restoration's performance and longevity [4,21–24]. Innovations in conservative dentistry, such as minimum invasive dentistry (MID), are directed towards realizing multifunctional restorative bio-interactive materials. Recently, Rabeia and Abdulla (2023) described a multifunctional RMGIC containing 2(methacryloxy) ethyl phosphate (2-MEP) and phosphorylated RMGIC (eRMGIC). It exhibited remarkable compressive and flexural strength and low solubility primarily owing to the presence of pendant phosphate groups [25]. However, the influence of such functionalization on the bonding ability of RMGIC's to different dental substrates has not yet justified. To the best of the authors knowledge and after reviewing of the literature, no research has been conducted on the modification of RMGIC with a phosphate functional monomer and this study is the first to examine the effect of adding 2-MEP to the liquid phase of resin modified glass ionomer luting cement on the bonding strength to different dental substrates.

Therefore, this study aimed to evaluate the effect of functionalizing chemically cured RMGIC by incorporating an organophosphorus monomer, 2-(methacryloxy)ethyl phosphate (2-MEP) which is a type of photoreactive and proton-conductive polymer based on phosphate monomers. Its pendant phosphate group is commonly utilized as an adhesive promoter. The dense matrix formed by the phosphate groups' interactions with their polarity enhances mechanical properties and increases resistance to water intrusion, resulting in decreased solubility and diffusion of water into the liquid part of the RMGIC (Fuji PLUS GC, USA). The 2-MEP had a concentration of 30 wt % of the liquid component of RMGIC. To fulfill the aim, we investigated the micro shear bond strength (μSBS) between four substrates (dentin, enamel, zirconia, and metal alloy) and three different luting cements. The null hypothesis was that the μSBS at the interface between the substrates and cement would not be affected by incorporating a phosphate-based co-monomer into the control cement (RMGIC).

2. Materials and methods

2.1. Substrates and cements with grouping

The main materials used in this study were Fuji PLUS (FP), modified Fuji PLUS (eRMGIC), and Rely X U200 self-adhesive resin (RU 200) cements. The material compositions of the luting cement and the substrates used to bond the cements are listed in Table 1.

The modified FP cement (eRMGIC) was obtained by incorporating 2-MEP into the liquid phase of the cement [25]. Experimental cement containing 2-MEP (30 wt %) was prepared according to Equation (1) [26]. 2-MEP (0.60 g, 30 wt%) was weighed using a digital balance with a precision of three decimal places. Subsequently, it was blended into 2 mL of the original cement liquid after subtracting the weight of the original liquid equivalent to that of the added monomer. The modified liquid was blended using a magnetic stirrer for 5 min to ensure a homogeneous dispersion [25,27].

$$Con = \frac{Wt}{V} \times 100 \quad (1)$$

where Con, Wt, and V denote the concentration (%), weight of the solute (g), and volume of the 100 mL solution, respectively.

Ninety-six specimens were created and categorized into four distinct groups based on the substrates used: human enamel, human dentin, zirconia, and metal alloys (A, B, C, and D). The substrates represent the different components of permanent restorations. Enamel and dentin represent the tooth structure (enamel and dentin), and zirconia and metal alloy are the most common materials for permanent restorations. The specimens were randomly subdivided into three subgroups (n = 8) (A1, A2, and A3; B1, B2, and B3; C1, C2, and C3; and D1, D2, and D3) based on the type of cement used: (1) FP, (2) eRMGIC, and (3) RU 200. G* power 3.0.10 (University of Kiel, Germany) was used to estimate the sample size (n = 8) allocated to each group. The statistical power and alpha error probability were set as 80 % and 0.05, respectively, for a two-sided test. The effect size of F was 0.4, which indicated a large effect [28].

Thirty maxillary premolar teeth, sourced from various health institutions, were extracted for orthodontic purposes to obtain enamel and dentin samples. The individuals from whom these teeth were obtained were aged between 14 and 30 years. The teeth were acquired from Diyala governorate and some private clinics in Dyala/Baqub'a city. The collection of teeth adhered to the guidelines outlined by the Research Ethics Committee of the College of Dentistry at the University of Baghdad (reference number 617 on 2-6-2022).

We ensured that the teeth were crack-free and healthy using 5× dental loupes. The dental surfaces were cleaned using pumice and a silicone cup. Subsequently, they were thoroughly rinsed using distilled water [29]. To prevent bacterial and fungal development, the teeth were placed in thymol solution (0.1 %) at a room temperature (20–25 °C) for a period of 60 d before the investigation [30,31].

2.2. Preparation of enamel samples

Six teeth were selected for microshear testing. The roots were excised and the crowns were sectioned longitudinally into buccal and

Table 1
Tested materials, type, composition, and batch numbers as per the manufacturer's descriptions.

Materials	Type	Composition	Lot No	Manufacturer
Fuji PLUS RMGIC (Control cement)	Chemical cure luting cement	Powder: fluoro aluminosilicate glass, pigment, initiator; Liquid: HEMA, tartaric acid, maleic acids, copolymer of acrylic and chemical initiators, water.	210713A	GC America, Chicago IL, USA
Modified Fuji PLUS (eRMGIC) (experimental cement)	Chemical cure luting cement	Powder: fluoro aluminosilicate glass, initiator, pigment; Liquid: 2-(methacryloxy) ethyl phosphate 30 %, HEMA, tartaric acid, maleic acids, copolymer of acrylic and chemical initiators, water.	210713A	GC America, Chicago IL, USA
Rely X U200	Self-adhesive resin cement	Base paste components: glass powder treated with silane, TEGDMA silane-treated silica, fiberglass, 2-methyl 1,1-[1 (hydroxymethyl)-1,2-ethanodiil] ester, 2-propenoic acid, *t*-butyl per-3,5,5-trimethyl hexanoate, and sodium persulfate Catalyst paste components: glass powder treated with silane dimethacrylate caption by substituted dimethacrylate, sodium *p*-toluenesulfonate, silane-treated silica calcium,1-benzyl-5-phenyl-acid barium salts, calcium hydroxide, and titanium dioxide 1,12-dodecane dimethacrylate	9065438	3 M ESPE, Seefeld, Germany
2-(methacryloxy)ethyl phosphate	Phosphate functional monomer	–	52628-03-2	Polysciences Europe GmbH, Germany
Zirconia	IPS e.max ZirCAD	87 % ZrO2, Y2O3, HfO2, Al2O3	X08278	Ivoclar Vivadent (Schaan, Liechstenstein)
Base metal alloy	Co–Cr powder alloy	62.69 % Co, 27%Cr, others 10 %		Cocrmow, Mti, China

palatal parts [32]. Four sections of enamel slabs were produced from the middle of the palatal and buccal surfaces of each tooth using an XP precision sectioning saw (Pelco, USA). Their measurements were verified using a digital caliper (Ningbo, China) to obtain accurate dimensions (approximately 3 mm length, 3 mm width, and 1.5 mm thick) and were marked using a ruler. A line was drawn from the tip of the buccal cusp to the cervical line, and another line was drawn between the mesial and distal tooth surfaces at their maximum prominent curvature to determine the middle area of the buccal and palatal surfaces (Fig. 1A–D) [33]. A silicone mold was used to embed the samples in acrylic resin by exposing the outer enamel surface and allowing it to set for 30 min using dental surveyor (Fig. 2A–D) [34]. To achieve flat surfaces, the samples were polished for 10 s using a polishing machine (Laryee Technology, China) equipped with 1200-grit silicon carbide abrasive sheets. Subsequently, a diamond paste was used to polish the samples (15 μm Diamond Paste, Struers) with water cooling employed until the enamel achieved a flattened surface [35].

2.3. Preparation of dentin samples

Acrylic blocks were constructed using a cylindrical silicone mold that was specifically created for this purpose. The cementoenamel junction (CEJ) was restricted, and an additional marking was created 2 mm apical to the CEJ to indicate the position of the teeth inside the acrylic material [36]. Following the manufacturer's guidelines, an acrylic resin (VERACIL, Colombia) with a cold cure was prepared and injected into the silicon mold, and both the buccal and palatal cusps were sectioned using an electrical diamond saw (Gamberini, Italy). The section was made 1.5 mm cervical to the mesial pit to expose a dentin surface for investigation. To determine ridge height, a periodontal probe was used to measure the distance from the pit to the mesial marginal ridge. This estimate was increased by 1.5 mm, and a mark was made on the mesial side of a tooth. Subsequently, the tooth was submerged in water and was cut with a saw to create a smooth horizontal surface [37].

A custom-made holder with a movable horizontal arm leveled dentin and enamel specimens to facilitate handling and for consistent polishing pressure.

The samples were leveled and finished using a grinder\ polisher device (MO pao 160E, China), first with a 600-grit paper under running water and subsequently with rotating aluminum oxide papers at a constant speed of 600 rpm for 60 s. This process aimed to obtain flat and smooth sample surfaces and to standardize the smear layer [38].

2.4. Preparation of zirconia samples

Twenty-four pre-sintered 3Y-TZP disks (5 mm diameter and 2 mm thickness) were designed using Google SketchUp software to create a standard tessellation language (STL) file. The disks were designed by importing the STL file to a software program (Exocad Dental CAD2.2, Exocad GmbH, Darmstadt, Germany). Dry milling was performed using the In-Lab MC X5 milling machine. The specimens were sintered in a furnace (InFire HTC speed sintering furnace, Sirona) following the cycle prescribed by the manufacturer (sintering temperature of 1650 °C for 8 h, and 90 min for cooling) [39,40]. After sintering, the zirconia specimens shrunk by 25 %, resulting in their final dimensions of 2 mm × 5 mm (height × diameter). All samples were embedded in a chemically cured methacrylate material using a cylindrical silicone mold specially designed for this purpose. (Fastray, HJ Bosworth, Skokie, IL, USA). A custom-made holder was then used to prepare the specimens using a grinder/polisher device (MO Pao 160E, China), first with a 600-grit paper under running water and subsequently with rotating aluminum oxide papers at a constant speed of 600 rpm for 60 s, to obtain flat and smooth surfaces and to standardize the smear layer [38]. The surfaces of all samples were then sandblasted using 53-μm aluminum oxide particles (Al_2O_3) (Aqua care powder, UK). A pressure of 1 bar was applied at a distance of 10 mm for 15 s between the nozzle and the surface of the specimens using a sandblast device (Aqua care device, UK) [41].

2.5. Preparation of metal samples

Co–Cr alloy specimens were created using selective laser melting (SLM). Twenty-four specimens were created with thickness and diameter of 2 mm and 5 mm, respectively. A 3D printing program (Lychee Slicer, 3D Mango, Belgium) was used to create the

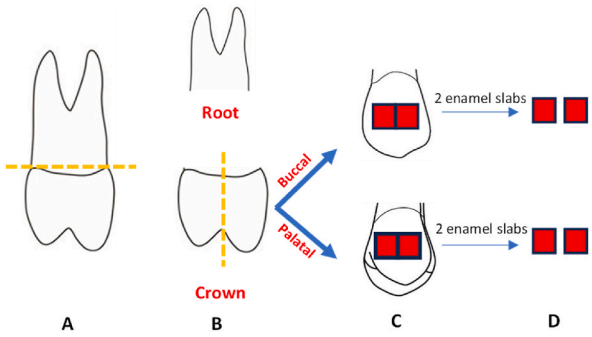

Fig. 1. Preparation of enamel slabs (A): Root was excised. (B): The crown separated longitudinally into the buccal and palatal parts. (C): The buccal and palatal surfaces. (D): Four sections of enamel slabs.

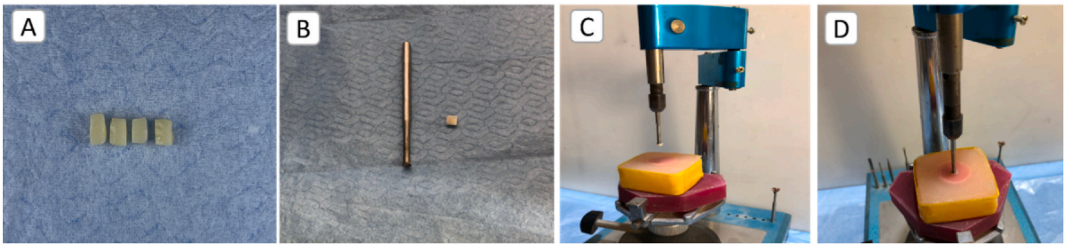

Fig. 2. Enamel sample preparation. (A): Enamel slaps. (B): Enamel slap with a metal rod. (C): Slaps attached to the vertical arm of dental surveyor. (D): Sample insertion into the silicone mold.

geometrical shape of the specimen, which was saved as an STL file. An SLM machine (D-150, Riton, China) was used to fabricate disk specimens [38,42]. The metal substrates were abraded with 53-μm Al_2O_3 (Aqua cure powder, UK) for 10 s in the sandblasting machine (Aqua care device, UK), with a distance of 10 mm between the samples and the source of particles [43]. Deionized water was used to clean and wash all the samples for 3 min to remove surface debris using an ultrasonic cleaner (model cd-4820, China) [38].

All the samples used in this study are shown in Fig. 3.

2.6. Cements application

For applying the FP and experimental cements, the enamel and dentin samples were conditioned using a citric acid conditioner (10 % for 20 s) in accordance with the manufacturer's recommendations and were then efficiently rinsed with water. Subsequently, gentle air (oil-free air) was blown to remove the excess water and obtain a glistering and moist surface. The samples used with RU200 did not require surface treatment except sandblasting.

Using Teflon as the primary material, a specific device was developed to establish a standardized approach for applying cement to the different substrates. The device was composed of a cylindrical structure designed to fit the acrylic block well. This cylindrical mold had a removable Teflon cover. The cover consisted of two 3-mm-thick half-circle pieces. The cover was attached to the cylinder using four screws. To connect the acrylic block to the Teflon cover, a detachable metal bar with a central screw was placed at the bottom of the cylindrical mold. Additionally, four screws were positioned around the cylinder to stabilize the acrylic block and direct the surface of the specimen towards a hole with a diameter of 2 mm in the Teflon cover. This hole was intended to receive polyethylene microtubes (as shown in Fig. 4A–F), which were obtained by cutting a 6-mm FG Nelaton catheter. These microtubes had a height and internal diameter of 3 mm and 1 mm, respectively, and were placed at the center of the Teflon mold [44,45].

The FP and experimental cements were mixed using hand-mixing glass powder with non-modified and modified liquids, respectively, as per the manufacturer's instructions at a relative humidity of (35.5 %) and at the temperature of 23 ± 2 °C. One large scoop of powder was dispensed to three drops of liquid. A three-digit analytical balance (Sf-400c, China) was used to weigh the powder and the three liquid drops (0.25 g ± 0.02 and 0.10 g ± 0.02, respectively) and to prevent the occurrence of proportional errors while preparing the samples. The liquid and powder were dispensed onto a mixing pad. The powder was divided into two equal portions, and the first portion was mixed with the liquid for 15 s. The remaining portion was added and mixed for 15–20 s (total mixing time: 30–40 s). The dispensing of the RU 200 cement was achieved using an auto-mixing tip owing to its paste-paste system.

The FP and experimental cements were inserted into the microtubules using a U-100 disposable insulin syringe (Dispovan, India) and the microtubules were cut at 20-unit intervals using a sharp cutter. The syringe was then loaded with the mixed cement and a plastic spatula. The syringe plunger was reinserted, and the cement was dispensed through the endodontic tip attached to the Luer lock connection of the syringe, which was precisely fitted to the internal lumen of the microtubules. The RU200 cement was dispensed using

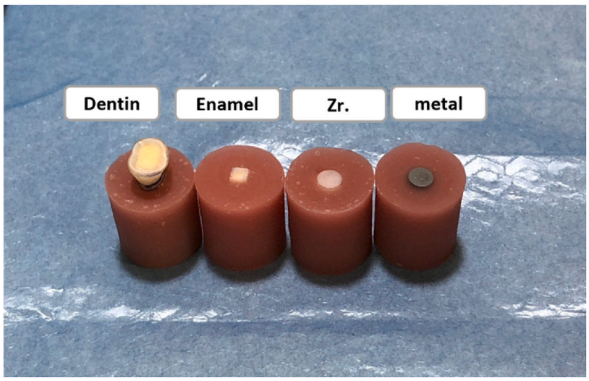

Fig. 3. Different samples used in this study.

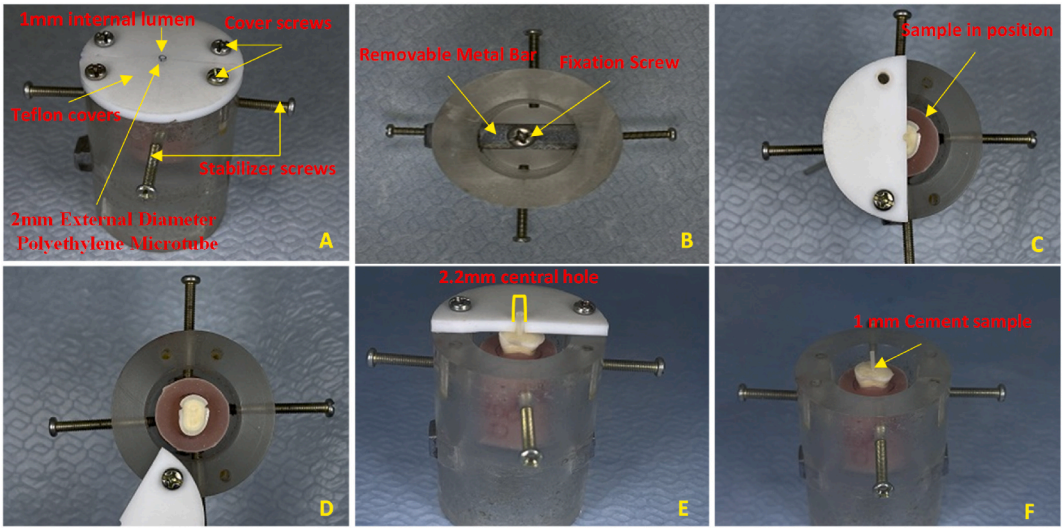

Fig. 4. Teflon Mold (A): Full view. (B): Bottom view. (C): Sample in place. (D): Top view of sample. (E): Side view of the sample with cement material within the polyethene microtubules. (F): Cement sample free from polyethylene microtubules.

a disposable auto-mixing tip connected to the endodontic tip [45].

In all samples, excess cement was removed from the periphery of the mold using a sharp explorer. To minimize the possibility of air bubble incorporation in the samples during dispensing, an EndoActivator (Dentsply Tulsa Dental, Tulsa, OK, USA) with a red tip (25/0.04) was used to agitate the cement at 10,000 cycles/min (167 Hz) for 5 s [46].

The FP and experimental cement samples were left for 4 min and 30 s, respectively, to obtain the initial setting time after dispensing, in accordance with the recommendations of the manufacturer. The RU200 samples were light-cured directly from the top of the mold at 1200 mW/cm^2 using LED curing unit (Bluephase Style, Ivoclar Vivadent) after the samples were dispensed in the tubule for 20 s [47]. After removing the RU 200 samples from the mold, they were further cured at two sites located at the edge of each sample (20 s), with each point perpendicular to the other, to achieve optimal sample curing.

All the samples were then released from the mold by untightening the four cover screws and the cylinder screws. At 37 °C, these samples were stored for 24 h in an incubator inside distilled water. Subsequently, each microtubule was carefully removed by making a vertical incision along its wall with a surgical blade of size 15, allowing the cement microcylinders to firmly adhere to the surfaces of various substrates [48]. The luting cement cylinders were then examined using 5× magnifying loupes (EyeMag Smart medical loupes from ZEISS, Jena, Germany). An LED light was used to examine the specimens to identify and eliminate any samples containing air bubbles or visible faults. However, no such specimens were detected, and all were considered well-suited for testing [47]. A blade was used to remove excess resin materials (flash) under the tube rim.

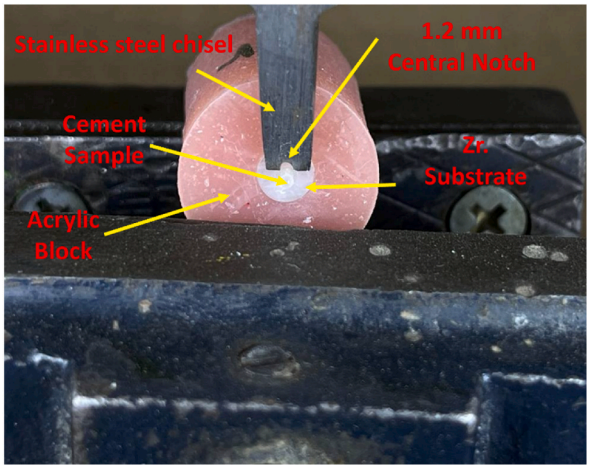

Fig. 5. Micro-Shear Test, Custom-made chisel specially designed for micro shear samples illustrates the micro shear test chisel, acrylic block with cement sample on Zirconia substrate.

2.7. Micro-shear bond strength testing

The micro-shear bond test involves the application of force to cylindrical cement samples that have adhered to the substrate discs, using a blade connected to a universal testing machine. The samples were placed in a jig affixed to the universal testing machine (Laryee, China) to determine their μSBSs. A custom-made notched chisel (central notch radius of 1.2 mm) mounted on the testing machine with a 5-kN load cell was used to apply the shear load to each specimen at a crosshead speed of 0.5 mm/min. The load was applied parallel to the direction of the bonded interface until the occurrence of failure (Fig. 5) [49]. Measurements of the 12 groups were conducted simultaneously using the same setup. To calculate μSBS, the maximum load was divided by the cross-sectional surface area [44].this test was done according to description in the ISO/TS 11405: 2015 [50].

The failure modes of the examined specimens were studied using scanning electron microscopy (SEM). (SEM, Axia ChemiSEM, Thermo Fisher Scientific, Waltham, MA, USA). The samples were first dried. They were then coated with gold nanoparticles for 2 min using a current of 45 mA and subsequently examined via SEM at an operating voltage of 30 kV. We used a working distance if 10–15.1 mm at a magnification of $\times$ 80. The failure modes in the substrate were categorized as adhesive, mixed mostly adhesive, mixed mainly cohesive, and cohesive [51].

2.8. Statistical analysis

Software for Windows version 25 (SPSS, Chicago, IL, USA) was used to statistically analyze the presented data. The Shapiro–Wilk test ($p > 0.05$) was used to evaluate the normality of the data. Statistical analysis was performed using two-way analysis of variance (ANOVA). The Tukey multiple comparison test was used ($p < 0.05$) to elucidate the effect of FP functionalization on the μSBS of each cement for all four substrates and the difference in the effect between the substrates.

3. Results

3.1. μSBS results

Table 2 and Fig. 6 show the μSBS of the samples 24 h after the application of the cements to different substrates. The results of the Shapiro–Wilk test revealed that the data were normally distributed. The results of the two-way ANOVA test revealed that, compared to the control FP and RU 200 cements, the FP cement exhibited a noticeable difference when functionalized with 30-wt.% 2-MEP.

In group A (cement applied to enamel), the subgroup A2 (eRMGIC) exhibited highest mean μSBS (18.6 $\pm$ 2.2). By contrast, the mean μSBS was significantly lower in subgroup A1 (FP) (10.8 $\pm$ 1.4) ($p < 0.001$). In group B (cement applied to dentin), the subgroup B3 (RU 200) exhibited the highest mean μSBS (20.4 $\pm$ 1.2). By contrast, subgroup B1 (FP) and B2 (eRMGIC) showed statistically significantly lower mean μSBS values of 8.8 $\pm$ 0.8 ($p < 0.001$) and 17.1 $\pm$ 0.9 ($p < 0.001$), respectively.

In group C (cement applied to Zirconia), the highest mean μSBS was observed in subgroup C3 (RU 200) (19.2 $\pm$ 1.9). By contrast, the lowest mean μSBS value was observed in subgroup C1(FP) (9.0 $\pm$ 1.0) ($p < 0.001$). The subgroup C2 (eRMGIC) showed statistically non-significant differences from subgroup C3 (RU 200) (18.1 $\pm$ 0.8, 19.2 $\pm$ 1.9) ($p > 0.05$).

In group D (cement applied to metal alloy), the highest mean μSBS was observed in subgroup D3 (RU 200) (15.8 $\pm$ 0.6), whereas the lowest mean μSBS was observed in D1 (FP) (8.0 $\pm$ 1) ($p < 0.001$). By contrast, the subgroup D2 (eRMGIC) exhibited statistically non-significant differences (14.2 $\pm$ 0.7) ($p > 0.05$) from D3 (RU 200).

Among the different groups, group A (enamel) exhibited the highest mean μSBS value of experimental cement (eRMGIC), whereas group D (metal alloy) exhibited the lowest.

3.2. Mode of failure

Fig. 7 shows the frequencies of the detected failure modes in various categories. For all groups (A, B, C, and D), adhesive failures were the most prevalent in the control subgroup (FP). Fig. 8a shows the SEM images illustrating the adhesive failure mode of FP when

Table 2
Mean micro-Shear bond strength (MPa), sample size, and standard deviations (MPa).

Substrates (Group)	**n	Mean (±*SD) Micro-Shear bond strength (MPa)		
		FP (subgroup 1)	eRMGIC (subgroup 2)	RU 200 (subgroup 3)
Enamel (A)	8	10.8 (1.4)^{Aa}	18.6 (2.2) ^{Ab}	18.0 (1.0) ^{Ab}
Dentin (B)	8	8.8 (0.8) ^{Ba}	17.1 (0.9) ^{Ab}	20.4 (1.2) ^{Bc}
Zirconia (C)	8	9.0 (1.0) ^{Ba}	18.1 (0.8) ^{Ab}	19.2 (1.9) ^{ABb}
Metal alloy (D)	8	8.0 (1.0) ^{Ba}	14.2 (0.7) ^{Bb}	15.8 (0.6) ^{Cb}

Similar lowercase letters in the same row represent no significant differences among the groups (ANOVA, post-hoc Tukey test at a significance level of $p = 0.05$).
Similar uppercase letters in the columns indicate nonsignificant differences among the different substrates for different luting cements.
* Standard deviation (SD) and.
** sample size.

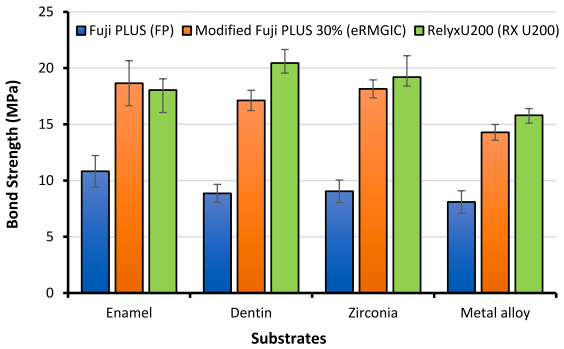

Fig. 6. Average μSBS (micro-shear bond strength) values in MPa for several luting cements when applied to different substrates and stored for 24 h in distilled water.

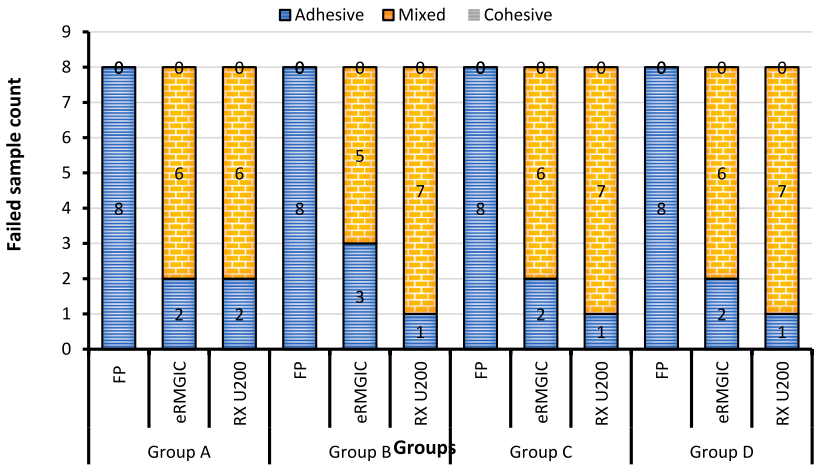

Fig. 7. Distribution of failure patterns in different specimen groups.

bonded to metal substrates. Across all groups, mixed failures (either mixed mainly adhesive or mixed mainly cohesive) were the most common failure mode in the eRMGIC subgroup. Fig. 8b shows the mixed mainly cohesive failure mode of eRMGIC on the enamel substrate, and Fig. 8c shows the mixed adhesive failure mode on metal substrates. Fig. 8d illustrates the adhesive failure mode of eRMGIC on the dentin substrate. As shown in Fig. 8e, for all groups, mixed failures (mainly cohesive) were the most frequent in the RU 200 subgroup on the zirconia substrate. However, for all groups, the pure adhesive failure modes of this cement exhibited the lowest frequencies.

4. Discussion

This study focused on the bonding efficacy of different luting agents (based on the functionalization of (self-adhesive RMGIC) luting cement (Fuji PLUS)) with other substrates (enamel, dentin, zirconia, and metal alloy).

SARCs were developed to avoid the need for separate etching, priming, and bonding procedures. The cements under consideration were prepared using novel combinations of monomers, fillers, and initiators. Incorporating an acidic monomer simplifies the process by consolidating the application of the adhesive and cement into one phase, eliminating the need for the prior three sequential stages. The acidic monomer, methacrylates with multifunctional phosphate groups, may interact with both HAp in hard tooth tissue and essential fillers of the luting cement. Restorative bio-interactive materials are the focus of innovations aimed at expanding their range of uses [7,52].

Rabeia and Abdulla (2023) [25] investigated the effect of adding 2-MEP, which contains a pendant phosphate group, to the liquid phase of the control cement FP for various percentages (0,10, 20, 30, and 40 % by weight) in different periods (1, 28, and 180 days) without any adjustments to cement powder phase. The results of this study revealed that the mean compressive and flexural strengths of the cement (eRMGIC) modified with 30 % 2-MEP were the higher than those of the control and other modified cements (10, 20, and 40 wt%), which exhibited low solubility after one month of immersion in distilled water [25].

From the aforementioned results given above, it can be concluded that, compared to FP, the modified cement eRMGIC exhibited

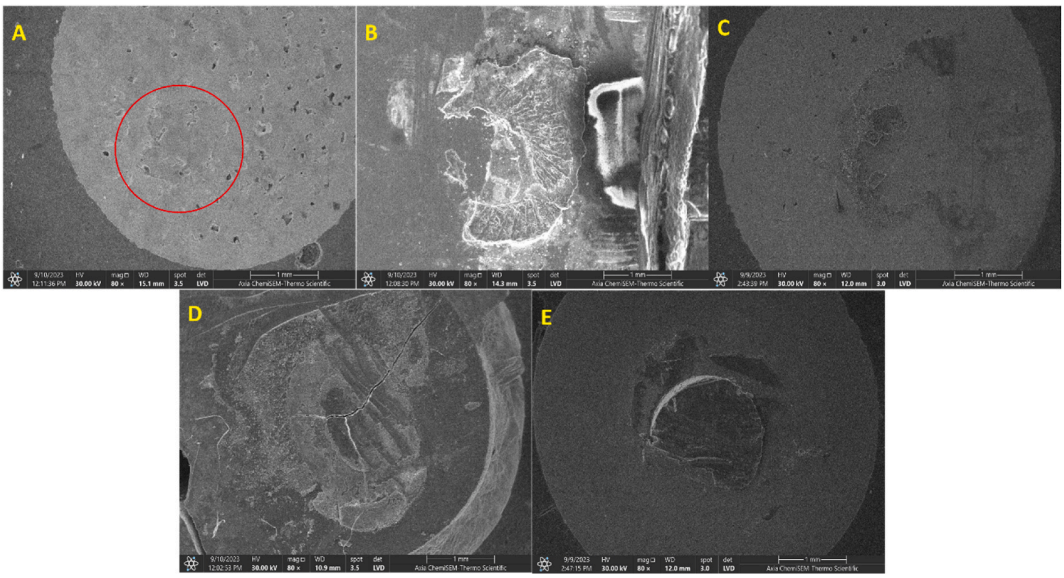

Fig. 8. Scanning electron micrographs of failure modes for different substrates at × 80 magnification and working distance of 10–15.1 mm. A. Adhesive failure mode of control cement FP on metal substrate (red circle); B. Mixed mainly cohesive failure mode of experimental cement eRMGIC on enamel substrate; C. Mixed mainly adhesive failure mode of experimental cement on metal substrate; D. Adhesive failure mode of experimental cement eRMGIC on dentin substrate; and E. Mixed mainly cohesive failure mode of RU 200 on zirconia substrate. (For interpretation of the references to colour in this figure legend, the reader is referred to the Web version of this article.)

noticeable performance enhancement following the functionalization of the tooth substrates (dentin and enamel) and restorative substrates (zirconia and metal alloy). This, in turn, can directly impact the long-term clinical performance of indirect restoration, which primarily depends on the integrity of the interface between the tooth structure and restoration. Therefore, the null hypothesis is rejected.

4.1. Bonding to enamel (group A)

According to the results of this study, the modified cement (eRMGIC) exhibited the highest μSBS. The acidic monomer introduced in the eRMGIC facilitated enhanced self-etching capabilities, resulting in greater exposure to enamel prisms and improved micromechanical retention. [53], This, in turn, increased the μSBS of eRMGIC (18.6 $\pm$ 2 MPa) compared to that of FP. This result is well-consistent with the previously published μSBS values for RMGICs (19.7 MPa) [54]. The functionality of the acidic monomer with carboxylic groups is expected to result in ionic bonding with calcium ions through chemical interactions, as reported for the interactions with polyalkenoic acid [55].

The results indicate that eRMGIC might chemically bond with enamel through a surface demineralization mechanism, improving μSBS compared to that of FP (10.8 $\pm$ 1.4) and making it comparable to that of RU 200 (18 $\pm$ 1 MPa). The results also revealed that RU 200 exhibited a satisfactory bond strength with enamel, as widely documented in the literature [56]. This could be attributed to the mechanism by which RU 200 bonds to the enamel. The functional monomer in RU 200 directly interacts by demineralizing and infiltrating tooth substrates, resulting in chemical and micromechanical retention [57]. This assumption is supported by the failure mode of eRMGIC, namely mixed failure (75 %), indicating the integration of cement with the exposed enamel prisms. By contrast, the FP cement exhibited adhesive failures (100 %) when bonded with enamel, owing to its porous internal structure and superficial hybridization of the interface.

4.2. Bonding to dentin (group B)

The self-adhesive properties of RMGICs allow them to attach nanomechanically to dentin by penetrating the exposed collagen network via pre-conditioning with 10 % polyacrylic acid (PAA). They can also attach chemically via the ionic interaction of polyalkenoic acid carboxyl groups with calcium [58]. The components of the glass ionomer penetrated the demineralized dentin and formed a bond by generating thin hybrid layers. Simultaneously, the carboxyl groups of PAA engage with Ca^{+2} ions in the residual HAp surrounding the collagen fibrils [58]. The practicality of RMGICs lies in their ability to create prolonged and immediate bonds with dentin, resulting in improved bond strength over time. This is attributed to their capacity to generate a uniform thin hybrid layer. However, notably, this characteristic is relevant only to the eRMGIC. This is due to the moderate acidity of the material, which selectively demineralizes only the extrafibrillar space surrounding the collagen fibrils. Consequently, it preserves the intrafibrillar apatite crystals near endogenous proteases and single fibrils, which can be recognized inside the hybrid layer [59]. The presence of the

acidic monomer in eRMGIC enhances its acidity compared to that of the original cement (17.1 ± 0.9 MPa) ($p < 0.001$), which induces additional demineralization at the dentine interface, rapidly enhancing the micromechanical bonding. Additionally, eRMGIC was initially hydrophilic. This is attributed to the polarity of the phosphate group and the availability of HEMA, which promoted the ionization of acidic groups when combined with a hydrated substrate. Consequently, the self-etching capability of the cement was enhanced, facilitating the penetration of the polymer in the substrate [4]. Water was expected to be reused throughout the eRMGIC setting process because of the reaction between the acidic functional groups and the ion-releasing essential filler particles. This enhanced the adaptability of eRMGIC to the tooth substrate and increased tolerance to moisture. Simultaneously, the failure mechanism from predominantly adhesive FP (100 %) to mixed patterns. (63.5 %).

In group B, the RU 200 subgroup exhibited the highest mean μSBS value; According to the "Adhesion-Decalcification" theory, the specific functional monomers present in RU 200 can engage in ionic interactions with HAp [60]. Phosphoric acid groups in multifunctional monomers simultaneously penetrate and demineralize dentin. Radical polymerization is the primary mode of the reaction and may be triggered by either a self-curing process or light exposure. Consequently, substantial cross-linking occurs among the cement generating polymers with higher molecular weights. It is speculated that the bond formed between the monomer acidic groups and the hydroxyapatite is responsible for the acquired adhesion via micromechanical retention and chemical interactions. The chemical bonding with HAp and micromechanical interlocking is believed to function synergistically to provide optimal material adhesion. In addition to the functional monomers, RU 200 contain additional essential components that contribute to its bonding ability. Rheological modifiers were incorporated into RU 200 to enhance its flowability, thereby potentially augmenting its wettability to the substrate. These strategies significantly enhanced the mean μSBS of RU 200 when bonded with dentin (20.4 ± 1.2) compared to those of FP and eRMGIC cements. This result can be logically explained using the failure mode of RU 200, which was predominantly mixed failure (87 %). The predominant failure modes in the FP and eRMGIC subgroups were (100 %) adhesive and (63.5 %) mixed failures, respectively.

4.3. Bonding to zirconia (group C)

The results indicated that eRMGIC exhibited a significantly higher mean μSBS (18.1 ± 0.8) than the control FP (9.0 ± 1). eRMGIC exhibited the most intense effect of functionalization of control cement. Conventional cements, such as glass ionomer cements and resin-modified glass ionomer cements, have been reported to exhibit weak bonding in zirconia. Despite the absence of phosphate ester monomers, the RMGIC can establish chemical and mechanical bonds with zirconia materials [61]. It has been proposed that the polyalkenoic acid polymers in these substances can undergo chemical reactions with metal oxides. The present findings are well-consistent with prior research findings, which demonstrate that resin-based self-adhesive cements exhibit superior bonding strengths compared to RMGICs when applied to diverse prosthetic substrates, including non-noble and noble alloys, glass-based ceramics, and zirconia [61].

The challenge of establishing an effective bond with zirconia may be attributed to the inert nature of the material. As zirconia is devoid of glass and silica, it resists acids, and silane coupling agents cannot create a siloxane network in its highly crystalline structure. Furthermore, it is difficult to produce a uniform micromechanical retention on its surface [62]. To solve the bonding issues associated with zirconia restorations, researchers have examined different surface treatment methods using both mechanical and chemical approaches. The most significant methodologies are the use of airborne-particle abrasion (APA), primers that contain acidic functional monomers, and SARCs, which include acidic functional monomers with either phosphate or carboxylate acid groups [63]. Successful bonding has been achieved through micromechanical bonding with Al_2O_3 particles using APA, followed by the application of cement containing MDP, which provides efficient chemical bonding [64]. Chemical bonds can be formed on the zirconia surface by treating the surface with monomers containing phosphate functional groups. This is attributed to the chemical interaction between the Zr and OH group on the zirconia surface and the P–OH group of the phosphate monomer [65]. Several authors have reported that the surface free energy (SEF) of the zirconia bonding surface is enhanced via APA [66]. Therefore, the high SFE results in an improved surface wettability, which induces efficient bond strength in zirconia [67].

In the current study, two factors determined the enhancement in the mean μSBS of eRMGIC to zirconia: the improvement achieved via micromechanical retention and the chemical interaction between the P–OH group in the phosphate monomer and the Zr–OH group in the surface of zirconia. The results also revealed that RU 200, a well-known self-adhesive cement, exhibited satisfactory μSBS, aligning with previous studies [68]. In RU 200, the availability of phosphoric methacrylate ester was sufficient for the formation of P–O–Zr bonds and for providing the requisite bond strength in zirconia, owing to the specific quantity of Zr–OH on the surface of zirconia [69].

The failure modes transitioned from 100 % adhesive in FP to 75 % in eRMGIC, indicating the effect of functionalizing the control cement. In addition, the failure mode results showed 87.5 % mixed failures in RU 200.

4.4. Bonding to a base metal alloy (group D)

In group D (base metal alloy), statistically significant differences in μSBS (14.2 ± 0.7) were observed in eRMGIC compared to the control cement FP (8.0 ± 1). This result is attributed to the bonding mechanism between the cement and the metal framework. In addition to altering the metal surface texture or chemistry via surface treatment, the oxides on the metal surface can serve as compound storage sites, strengthening the chemomechanical interaction between the metal and adhesive cement.

APA is the most commonly used technique for enhancing micromechanical retention using Al_2O_3 particles [70]. This approach can potentially enhance the adhesive interaction between the substrate and cement by eliminating surface debris and augmenting the

surface roughness. These effects are accompanied by an increase in SFE and the formation of oxide framing. Co–Cr alloys with high Cr content provide evidence to support this hypothesis [71].

As reported by Salonga et al. [72], Cr generates chromium oxide, which forms stronger bonds than those made by other metal oxides. According to Capa et al., 2009, the bond strength of resin cement, or RMGIC, is higher than that of base metal alloys and noble metals [73].

In this study, an enhanced bond strength was observed between the base metal alloy and eRMGIC. This enhancement can be attributed to the incorporation of 2-MEP, which provides a strong and efficient interaction with metallic materials, creating a firm enduring bond [71]. This ability of the compound is primarily attributed to its constitution, specifically the presence of a dihydrogen phosphate group, which acts as an etching agent. The presence of water may lead to the dissociation of the substance into hydrogen ions (H+). Organic ester monomers can form covalent bonds with oxide layers formed on metal surfaces. Additionally, they can achieve mechanical retention on sandblasted surfaces [74].

In this study, the self-adhesive resin cement RU 200 also exhibited an enhanced bonding strength with the base metal alloy. This is attributed to the composition of the cement: it contains phosphoric acid ester as a functional monomer, which binds to the metal surface according to the mechanism mentioned previously. In addition, the high SFE and the roughening of the surface via sandblasting contributed to this excellent outcome [75]. The organic esters in RU 200 contain dihydrogen phosphate groups that disintegrate into two H^+ ions, in contrast to eRMGIC, where only one H^+ ion is released. The two H^+ ions then covalently bond to the oxide layer of the metal alloy [76].

Group D did not exhibit any cohesive failures in any subgroups. The high statistically significant difference observed in the eRMGIC subgroup compared to the FP subgroup can be explained using the failure modes of the subgroups, which were 75 % mixed and 100 % adhesive failures, respectively. RU 200 exhibited 87.5 % mixed failures, which explained the failure mechanism of RelyX-type cements.

4.5. Future work and limitations

The limitations of this study and future work are described below.

1. It is impossible to completely avoid differences in tooth structure, patient age, and difficulties in preparing zirconia and metal samples.
2. Using similar approaches, the μSBS performance of luting materials attached to the restorative material and tooth structure in vivo and its relationship to their mechanical performances should be studied.
3. The μSBS of all samples was measured within 24 h owing to the limited time available for this study. Hence, it is highly recommended for future studies to investigate the effect of aging on SBS, along with the changes in the mineral profile of luted teeth at the interface using XPS, surface microhardness, XRD, and Raman microscopy.
4. For further study, micro-tensile bond strength (μTBS) and interfacial fracture toughness (iFT) tests are recommended to measure the interfacial adhesion-tooth strength.

5. Conclusion

Within the limitations of this study, the following conclusions may be drawn.

1. The functionalization of RMGIC FP with a phosphate-based co-monomer (2-MEP) effectively enhances the μSBS of the modified cement eRMGIC compared to that of the control cement FP on different types of substrates (dentin, enamel, zirconia, and metal).
2. The modified cement exhibited the highest on enamel than on other tested cements (FP and RU 200).
3. Compared to RU 200 cement, eRMGIC cement exhibited comparable results on zirconia, and metal. However, it showed lower μSBS on dentin.
4. eRMGIC and RU 200 cements showed mixed-type failure for all substrates, whereas the FP cement exhibited pure adhesive failures on all substrates.
5. Despite the time constraints of the study, its findings provide fresh insights into the potential development of effective substances for optimum clinical use. Additional valuable information can be obtained through further research, including long-term studies and various tests, such as micro-hardness or micro-tensile tests.

Data availability statement

Data will be made available on request.

Funding

The study is self-funded.

Additional information

No additional information is available for this paper.

CRediT authorship contribution statement

Rabeia J. Khalil: Writing – review & editing, Writing – original draft, Visualization, Validation, Software, Resources, Methodology, Investigation, Funding acquisition, Formal analysis, Data curation, Conceptualization. **Abdulla M.W. Al-Shamma:** Visualization, Validation, Supervision, Project administration, Methodology, Conceptualization.

Declaration of competing interest

The authors declare that they have no known competing financial interests or personal relationships that could have appeared to influence the work reported in this paper.

Acknowledgements

The authors acknowledge the support from the University of Baghdad, Baghdad, Iraq. The authors also express their gratitude to the staff of the Materials Engineering Department at the University of Technology and the Ministry of Science and Technology for their collaboration.

References

[1] S.M. Morgano, C.W. VanBlarcom, K.J. Ferro, D.W. Bartlett, The history of the glossary of prosthodontic terms, J. Prosthet. Dent (2018), https://doi.org/10.1016/S0022-3913(99)70234-9.
[2] D.K. Zeller, J. Fischer, N. Rohr, Viscous behavior of resin composite cements, Dent. Mater. J. 40 (1) (2021) 253–259, https://doi.org/10.4012/dmj.2019-313.
[3] A.Y. Alsaeed, Bonding CAD/CAM materials with current adhesive systems: an overview, The Saudi Dental Journal 34 (4) (2022) 259–269, https://doi.org/10.1016/j.sdentj.2022.03.005.
[4] G.K.-H. Leung, A.W.-Y. Wong, C.-H. Chu, O.Y.J.D.J. Yu, Update on dental luting materials, Dent. J. 10 (11) (2022) 208, https://doi.org/10.3390/dj10110208.
[5] N. Baig, S. Khiyani, S. Meshram, M. Mhaske, N. Parasrampuria, V. Jadhav, Retentive properties of luting cements: a review, Clin. Dent. 9 (5) (2015), 10.3390%2Fmolecules28041619.
[6] M. Yoshioka, Y. Yoshida, S. Inoue, P. Lambrechts, G. Vanherle, Y. Nomura, M. Okazaki, H. Shintani, B. Van Meerbeek, Adhesion/decalcification mechanisms of acid interactions with human hard tissues, J. Biomed. Mater. Res.: An Official Journal of The Society for Biomaterials and The Japanese Society for Biomaterials 59 (1) (2002) 56–62, https://doi.org/10.1002/jbm.1216.
[7] L. Al-Taee, A. Banerjee, S. Deb, In-vitro adhesive and interfacial analysis of a phosphorylated resin polyalkenoate cement bonded to dental hard tissues, J. Dent. 118 (2022) 104050, https://doi.org/10.1016/j.jdent.2022.104050.
[8] S.A. Yamakami, A.L.M. Ubaldini, F. Sato, A. Medina Neto, R.C. Pascotto, M.L.J.J.o.A.O.S. Baesso, Study of the chemical interaction between a high-viscosity glass ionomer cement and dentin, J. Appl. Oral Sci. 26 (2018) e20170384, https://doi.org/10.1590/1678-7757-2017-0384.
[9] S. Sauro, V. Faus-Matoses, I. Makeeva, J.M. Nuñez Martí, R. González Martínez, J.A. García Bautista, V.J.M. Faus-Llácer, Effects of polyacrylic acid pre-treatment on bonded-dentine interfaces created with a modern bioactive resin-modified glass ionomer cement and subjected to cycling mechanical stress, Materials 11 (10) (2018) 1884, https://doi.org/10.3390/ma11101884.
[10] F. Sharafeddin, Z. Jowkar, S. Bahrani, Comparison between the effect of adding microhydroxyapatite and chitosan on surface roughness and Microhardness of resin modified and conventional glass ionomer cements, Journal of Clinical and Experimental Dentistry 13 (8) (2021) e737, 10.4317%2Fjced.55996.
[11] L. Al-Taee, S. Deb, A. Banerjee, An in vitro assessment of the physical properties of manually-mixed and encapsulated glass-ionomer cements, BDJ open 6 (1) (2020) 12, https://doi.org/10.1038/s41405-020-0040-x.
[12] D. Dionysopoulos, O. Gerasimidou, C.J.R.P.i.M. Papadopoulos, Modifications of glass ionomer cements using nanotechnology: recent advances, Recent Progress in Materials 4 (2) (2022) 1–22, https://doi.org/10.21926/rpm.2202011.
[13] Z.R. Hasan, N.R. Al-Hasani, O.J.J.o.B.C.o.D. Malallah, Color stability of nano resin-modified glass Ionomer restorative cement after acidic and basic medications challenge, Baghdad College of Dentistry 35 (4) (2023) 10–19, https://doi.org/10.26477/jbcd.v35i4.3505.
[14] H. Jamal, A Novel Atraumatic Self-Bonding and Self-Healing Dental Composite to Restore Carious Primary Dentition, UCL, University College London), 2021. https://discovery.ucl.ac.uk/id/eprint/10136353.
[15] M. Toledano, R. Osorio, E. Osorio, I. Cabello, M. Toledano-Osorio, F.S.J.J.o.d. Aguilera, In vitro mechanical stimulation facilitates stress dissipation and sealing ability at the conventional glass ionomer cement-dentin interface, J. Dent. 73 (2018) 61–69, https://doi.org/10.1016/j.jdent.2018.04.006.
[16] Y. Xie, R. Chen, W. Yao, L. Ma, B.J.B.P. Li, E. Express, Synergistic effect of ion-releasing fillers on the remineralization and mechanical properties of resin–dentin bonding interfaces, Biomedical Physics & Engineering Express 9 (6) (2023) 062001, https://doi.org/10.1088/2057–1976/ad0300.
[17] N.K. Mann, G.K. Chahal, J.S. Gil, S. Kainth, M. Sachdeva, S. Verma, G.K. Chahal II, J.S. Gill II, Evaluation of bond strength of resin and non-resin cements to different alloys, Cureus 15 (3) (2023), https://doi.org/10.7759/cureus.36894.
[18] T. Maravić, C. Mazzitelli, E. Mancuso, F. Del Bianco, U. Josić, M. Cadenaro, L. Breschi, A. Mazzoni, Resin composite cements: current status and a novel classification proposal, J. Esthetic Restor. Dent. (2023), https://doi.org/10.1111/jerd.13036.
[19] A. Malysa, J. Wezgowiec, W. Grzebieluch, D.P. Danel, M.J.I.J.o.M.S. Wieckiewicz, Effect of thermocycling on the bond strength of self-adhesive resin cements used for luting CAD/CAM ceramics to human dentin, Molecular Sciences 23 (2) (2022) 745, https://doi.org/10.3390/ijms23020745.
[20] A. Heboyan, A. Vardanyan, M.I. Karobari, A. Marya, T. Avagyan, H. Tebyaniyan, M. Mustafa, D. Rokaya, A. Avetisyan, Dental luting cements: an Updated comprehensive review, Molecules 28 (4) (2023) 1619, https://doi.org/10.3390/molecules28041619.
[21] C. Sabatini, M. Patel, E.J.O.d. D'Silva, In vitro shear bond strength of three self-adhesive resin cements and a resin-modified glass ionomer cement to various prosthodontic substrates, Operat. Dent. 38 (2) (2013) 186–196, https://doi.org/10.2341/11-317-l.
[22] S.-E. Lee, J.-H. Bae, J.-W. Choi, Y.-C. Jeon, C.-M. Jeong, M.-J. Yoon, J.-B.J.M. Huh, Comparative shear-bond strength of six dental self-adhesive resin cements to zirconia, Materials 8 (6) (2015) 3306–3315, https://doi.org/10.3390/ma8063306.
[23] V.J. Vivek, P. Venugopal, N. Divakar, S. Bharath, K. Sarin, N. Mohammed, Comparison of zirconia to dentin bonding using resin-based luting cements and resin-modified glass-ionomer cement: in vitro, J. Pharm. BioAllied Sci. 14 (Suppl 1) (2022) S460–S463, https://doi.org/10.4103/jpbs.jpbs_779_21.
[24] E.P. Maño, R.M. Algarra, A. Fawzy, V.C. Leitune, F.M. Collares, V. Feitosa, S.J.A.S. Sauro, In vitro bonding performance of modern self-adhesive resin cements and conventional resin-modified glass ionomer cements to prosthetic substrates, Appl. Sci. 10 (22) (2020) 8157, https://doi.org/10.3390/app10228157.

[25] R.J. Khalil, A.M. Al-Shamma, Physicomechanical Characterization of a novel resin-modified glass ionomer luting cement functionalized with a phosphate functional monomer, International Journal of Dentistry 2023 (2023), https://doi.org/10.1155/2023/6533954.
[26] D.A. Skoog, D.M. West, F.J. Holler, S.R. Crouch, Fundamentals of Analytical Chemistry, Cengage learning, 2013, https://doi.org/10.1021/ed040p614.2.
[27] D. Lee, H. Bae, J. Ahn, T. Kang, D.-G. Seo, D.S. Hwang, Catechol-thiol-based dental adhesive inspired by underwater mussel adhesion, Acta Biomater. 103 (2020) 92–101, https://doi.org/10.1016/j.actbio.2019.12.002.
[28] J. Cohen, Statistical Power Analysis for the Behavioral Sciences, Routledge, 2013, https://doi.org/10.4324/9780203771587.
[29] I.M. Hamouda, S.H. Shehata, Fracture resistance of posterior teeth restored with modern restorative materials, Journal of biomedical research 25 (6) (2011) 418–424, https://doi.org/10.1016/S1674-8301(11)60055-9.
[30] A. Secilmis, E. Dilber, N. Ozturk, F.G. Yilmaz, The effect of storage solutions on mineral content of enamel, Mater. Sci. Appl. 4 (2013) 439–445. http://www.scirp.org/journal/PaperInformation.aspx?PaperID=33843.
[31] B. Aydın, T. Pamir, A. Baltaci, M.N. Orman, T.J.E.j.o.d. Turk, Effect of storage solutions on microhardness of crown enamel and dentin, European journal of dentistry 9 (2) (2015) 262–266, https://doi.org/10.4103/1305-7456.156848.
[32] A.S. Bakry, M.A. Abbassy, Increasing the efficiency of CPP-ACP to remineralize enamel white spot lesions, J. Dent. 76 (2018) 52–57, https://doi.org/10.1016/j.jdent.2018.06.006.
[33] S.S. Rahee, R.H.J.J.o.B.C.o.D. Jehad, Comparing the effectiveness of using three different re-mineralizing pastes on remineralisation of artificially induced white spot lesion, Journal of Baghdad College of Dentistry 35 (4) (2023) 35–45, https://doi.org/10.26477/jbcd.v35i4.3512.
[34] J. Zhang, Therapeutic Effect of Chitosan on Remineralisation of Enamel Carious Lesions by Bioglass-Based Biomaterials, King's College London, 2018. https://kclpure.kcl.ac.uk/ws/portalfiles/portal/101484772/2018_Zhang_Jing_1478191_ethesis.pdf.
[35] L.A. Costa, K.K. Carneiro, A. Tanaka, D.M. Lima, J. Bauer, Evaluation of pH, ultimate tensile strength, and micro-shear bond strength of two self-adhesive resin cements, Braz. Oral Res. 28 (2014) 1–7, https://doi.org/10.1590/1807-3107BOR-2014.vol28.0055.
[36] S. Tohidkhah, E. Ahmadi, M. Abbasi, R.M. Farimani, L.R.J.B.R.I. Omrani, Effect of bioinductive cavity liners on shear bond strength of dental composite to dentin, BioMed Res. Int. 2022 (2022), https://doi.org/10.1155/2022/3283211.
[37] R.J. Khalil, A.M. Al-Shamma, Early and delayed effect of 2% chlorhexidine on the shear bond strength of composite restorative material to dentin using a total etch adhesive, Journal of Baghdad College of Dentistry 325 (2219) (2015) 1–17, https://doi.org/10.0001/707.
[38] R.A. Abuljadayel, Evaluation of a Dentine Hybrid Self-Adhesive Restorative Material Interface, King's College London, 2019. https://kclpure.kcl.ac.uk/ws/portalfiles/portal/108532805/2019_Abuljadayel_Roaa_1459502_ethesis.pdf.
[39] F.K. Ghadeer, L.E. Alwan, A.K.J.J.J.o.B.C.o.D. Al-Azzawi, Crystallization firing effect on the marginal discrepancy of the IPS. emax CAD crowns using two different CAD/CAM systems, Journal of Baghdad College of Dentistry 35 (1) (2023) 49–57, https://doi.org/10.26477/jbcd.v35i1.3316.
[40] T. Akar, A. Dündar, Ö. Kırmalı, Ö. Üstün, A. Kapdan, H. Er, A. Kuştarcı, K. Er, B.J.D. Yilmaz, m. problems, Evaluation of the shear bond strength of zirconia to a self-adhesive resin cement after different surface treatment, Dental and medical problems 58 (4) (2021) 463–472, https://doi.org/10.17219/dmp/135652.
[41] M.I. Abdulazeez, M.A. Majeed, Fracture strength of monolithic zirconia crowns with modified vertical preparation: a comparative in vitro study, European Journal of Dentistry 16 (1) (2022) 209–214, https://doi.org/10.1055/s-0041-1735427.
[42] I.H.H. Abbas Hamad Ghadhban, Transverse strength and Microstructure of cobalt-chromium alloy produced by selective laser melting and casting techniques, J. Res. Med. Dent. Sci. 11 (1) (2023) 176–182. https://www.jrmds.in/abstract/transverse-strength-and-microstructure-of-cobaltchromium-alloy-produced-by-selective-laser-melting-and-casting-technique-98115.html.
[43] S. Lawaf, S. Nasermostofi, M. Afradeh, A. Azizi, Comparison of the bond strength of ceramics to Co-Cr alloys made by casting and selective laser melting, The Journal of Advanced Prosthodontics 9 (1) (2017) 52–56, 10.4047%2Fjap.2017.9.1.52.
[44] M.M. Awad, N. Almutairi, F. Alhalabi, A. Robaian, F.A. Vohra, M. Ozcan, A. Maawadh, A. Alrahlah, Influence of surface conditioning on the repair strength of bioactive restorative material, J. Appl. Biomater. Funct. Mater. 18 (2020) 2280800020926615, https://doi.org/10.1177/2280800020926615.
[45] S.J. Jassim, M.A.J.H. Majeed, Effect of plasma surface treatment of three different CAD/CAM materials on the micro shear bond strength with resin cement (A comparative in vitro study), Heliyon 9 (7) (2023) e17790, https://doi.org/10.1016/j.heliyon.2023.e17790.
[46] Y.-L. Chen, H.-H. Chang, Y.-C. Chiang, C.-P. Lin, Application and development of ultrasonics in dentistry, J. Formos. Med. Assoc. 112 (11) (2013) 659–665, https://doi.org/10.1016/j.jfma.2013.05.007.
[47] M.D.S. Lanza, M.R.B. Andreeta, T.A. Pegoraro, L.F. Pegoraro, R.M.D. Carvalho, Influence of curing protocol and ceramic composition on the degree of conversion of resin cement, J. Appl. Oral Sci. 25 (2017) 700–707, https://doi.org/10.1590/1678-7757-2016-0270.
[48] M.A. ElGendy, I. Mosleh, H. Zaghloul, Micro-shear bond strength of bioactive cement to translucent zirconia after thermocycling: a comparative in-vitro study, Brazilian Dental Science 23 (1) (2020), https://doi.org/10.14295/bds.2020.v23i1.1830, 9 pp.-9.
[49] A.M. Ismail, C. Bourauel, A. ElBanna, T.J.D.J. Salah Eldin, Micro versus macro shear bond strength testing of dentin-composite interface using chisel and wireloop loading techniques, Dent. J. 9 (12) (2021) 140, https://doi.org/10.3390/dj9120140.
[50] P. Iso, Geneva, Switzerland, TS 11405: 2015, dentistry. Testing of Adhesion to Tooth Structure, 2015. https://scholar.google.com/scholar?hl=ar&as_sdt=0,5&q=PROOfS+ISO,+Geneva,+Switzerland,+TS+11405:+2015,+Dentistry.+Testing+of+adhesion+to+tooth+structure,+(2015).
[51] E.S. Marchenko, K.M. Dubovikov, G.A. Baigonakova, I.I. Gordienko, A.A. Volinsky, Surface structure and properties of hydroxyapatite coatings on NiTi substrates, Coatings 13 (4) (2023) 722, https://doi.org/10.3390/coatings13040722.
[52] B. Van Meerbeek, K. Yoshihara, K. Van Landuyt, Y. Yoshida, M.J.J.o.A.D. Peumans, From Buonocore's pioneering acid-etch technique to self-adhering restoratives. A status perspective of rapidly advancing dental adhesive technology, J. Adhesive Dent. 22 (1) (2020) 7–34, https://doi.org/10.3290/j.jad.a43994.
[53] E.A. Münchow, A.F. da Silva, G. da Silveira Lima, T. Wulff, M. Barbosa, F.A. Ogliari, E. Piva, Polypropylene glycol phosphate methacrylate as an alternative acid-functional monomer on self-etching adhesives, J. Dent. 43 (1) (2015) 94–102, https://doi.org/10.1016/j.jdent.2014.11.005.
[54] E.A. Glasspoole, R.L. Erickson, C.L. Davidson, Effect of surface treatments on the bond strength of glass ionomers to enamel, Dent. Mater. 18 (6) (2002) 454–462, https://doi.org/10.1016/s0109-5641(01)00068-9.
[55] R. Wang, Y. Shi, T. Li, Y. Pan, Y. Cui, W.J.J.o.d. Xia, Adhesive interfacial characteristics and the related bonding performance of four self-etching adhesives with different functional monomers applied to dentin, J. Dent. 62 (2017) 72–80, https://doi.org/10.1016/j.jdent.2017.05.010.
[56] J. Fehrenbach, E.A. Münchow, C.P. Isolan, L.P. Brondani, C.D. Bergoli, Structural reliability and bonding performance of resin luting agents to dentin and enamel, Int. J. Adhesion Adhes. 107 (2021) 102863, https://doi.org/10.1016/j.ijadhadh.2021.102863.
[57] S. Makkar, N. Malhotra, Self-adhesive resin cements: a new perspective in luting technology, Dent. Update 40 (9) (2013) 758–768, https://doi.org/10.12968/denu.2013.40.9.758.
[58] S.L. Sreejith, M.J.M.A. Saraswathy, Modifications of polyalkenoic acid and its effect on glass ionomer cement, Materials Advances (2024), https://doi.org/10.1039/D3MA00406F.
[59] S. Sauro, D.H. Pashley, Strategies to stabilise dentine-bonded interfaces through remineralising operative approaches–State of the Art, Int. J. Adhesion Adhes. 69 (2016) 39–57, https://doi.org/10.1016/j.ijadhadh.2016.03.014.
[60] B. Van Meerbeek, K. Yoshihara, Y. Yoshida, A. Mine, J. De Munck, K. Van Landuyt, State of the art of self-etch adhesives, Dent. Mater. 27 (1) (2011) 17–28, https://doi.org/10.1016/j.dental.2010.10.023.
[61] L. Yang, H. Xie, H. Meng, X. Wu, Y. Chen, H. Zhang, C. Chen, Effects of luting cements and surface conditioning on composite bonding performance to zirconia, J Adhes Dent 20 (6) (2018) 549–558, https://doi.org/10.3290/j.jad.a41634.
[62] D.Y. Toyama, L.M.M. Alves, G.F. Ramos, T.M.B. Campos, G. de Vasconcelos, A.L.S. Borges, R.M.J.J.o.t.m.b.o.b.m. de Melo, Bioinspired silica-infiltrated zirconia bilayers: strength and interfacial bonding, J. Mech. Behav. Biomed. Mater. 89 (2019) 143–149, https://doi.org/10.1016/j.jmbbm.2018.09.013.
[63] I.M. Garcia, J. Soto-Montero, F.M. Collares, M. Giannini, Bonding of resin cements to ultra-translucent zirconia after aging for 24 hours and 1 year, Int. J. Prosthod. 35 (4) (2022), https://doi.org/10.11607/ijp.7703.
[64] A.K.M. Tashkandi, The Effect of Zirconia Surface Treatment on Bond Strength of Various Cement Systems, Boston University, 2021. https://hdl.handle.net/2144/42846.

[65] R. Grasel, M. Santos, H.C. Rêgo, M. Rippe, L. Valandro, Effect of resin luting systems and alumina particle air abrasion on bond strength to zirconia, Operat. Dent. 43 (3) (2018) 282–290, https://doi.org/10.2341/15-352-l.
[66] N. Lümkemann, M. Eichberger, B. Stawarczyk, Different surface modifications combined with universal adhesives: the impact on the bonding properties of zirconia to composite resin cement, Clin. Oral Invest. 23 (2019) 3941–3950. https://link.springer.com/article/10.1007/s00784-019-02825-z.
[67] R.B.W. Lima, S.C. Barreto, N.M. Alfrisany, T.S. Porto, G.M. De Souza, M.F. De Goes, Effect of silane and MDP-based primers on physico-chemical properties of zirconia and its bond strength to resin cement, Dent. Mater. 35 (11) (2019) 1557–1567, https://doi.org/10.1016/j.dental.2019.07.008.
[68] C.T.R. Lago, B.L.T. Lago, J.P. De Carli, A. Paula, Influence of ceramic primers on microshear bond strength to zirconia, Biosci. J. 38 (2022) e38035, https://doi.org/10.14393/BJ-v38n0a2022-59850, 1981-3163.
[69] N. Passia, M. Mitsias, F. Lehmann, M. Kern, Bond strength of a new generation of universal bonding systems to zirconia ceramic, J. Mech. Behav. Biomed. Mater. 62 (2016) 268–274, https://doi.org/10.1016/j.jmbbm.2016.04.045.
[70] B. Śmielak, L. Klimek, K. Krześniak, Effect of sandblasting parameters and the type and hardness of the material on the number of embedded Al2O3 grains, Materials 16 (13) (2023) 4783, https://doi.org/10.3390/ma16134783.
[71] L. Sadighpour, A.S. Mostafavi, M. Pirmoradian, F. Alipuryalda, Comparison of bond strength in the different class of resin cements to cast and CAD/CAM Co-Cr alloys, International Journal of Dentistry 2021 (2021), https://doi.org/10.1155/2021/7843979.
[72] J.P. Salonga, H. Matsumura, K. Yasuda, Y. Yamabe, Bond strength of adhesive resin to three nickel-chromium alloys with varying chromium content, J. Prosthet. Dent 72 (6) (1994) 582–584, https://doi.org/10.1016/0022-3913(94)90288-7.
[73] N. Capa, Z. Özkurt, C. Canpolat, E. Kazazoglu, Shear bond strength of luting agents to fixed prosthodontic restorative core materials, Aust. Dent. J. 54 (4) (2009) 334–340, https://doi.org/10.1111/j.1834-7819.2009.01159.x.
[74] K.L. Van Landuyt, J. Snauwaert, J. De Munck, M. Peumans, Y. Yoshida, A. Poitevin, E. Coutinho, K. Suzuki, P. Lambrechts, B. Van Meerbeek, Systematic review of the chemical composition of contemporary dental adhesives, Biomaterials 28 (26) (2007) 3757–3785, https://doi.org/10.1016/j.biomaterials.2007.04.044.
[75] I.C.S. Ervolino, V.A.A. Bento, J.L. Brunetto, L. Bfcvm, I.S. Arantes, D.B. Castillo, Comparison of 3-and 90-day bond strengths of 3 types of cement to nickel-chromium alloy, Gen. Dent. 70 (1) (2022) 30–33. https://pubmed.ncbi.nlm.nih.gov/34978987/.
[76] F. Shafiei, M. Behroozibakhsh, A. Abbasian, S. Shahnavazi, Bond strength of self-adhesive resin cement to base metal alloys having different surface treatments, Dent. Res. J. 15 (1) (2018) 63, https://doi.org/10.4103/1735-3327.223610.